



Ionospheric Disturbances and Their Impacts on HF Radio Wave Propagation

Qiang Guo⁽¹⁾, Leonid F. Chernogor^(1,2), Konstantin P. Garmash⁽²⁾, Yiyang Luo⁽²⁾, Victor T. Rozumenko^{*(2)}, and Yu Zheng⁽³⁾

(1) Harbin Engineering University, People’s Republic of China

(2) V. N. Karazin Kharkiv National University, Kharkiv, Ukraine

(3) Qingdao University, People’s Republic of China

Abstract

The multi-frequency multipath observations of temporal variations in the Doppler spectra and signal amplitudes of HF radio waves reflected from the ionosphere, which accompanied ionospheric disturbances caused by an ionospheric storm, an earthquake, and a solar eclipse, are described. Aperiodic and quasi-periodic disturbances have been detected in the radio signal and ionospheric parameters.

1 Introduction

This paper deals with temporal variations observed in the Doppler spectra and signal amplitudes of HF radio waves during the 25 – 26 August 2018 ionospheric storm, the 5 September 2018 Japan earthquake, and the 11 August 2018 solar eclipse.

2 Instrumentation

To analyze how ionospheric perturbations arising from various sources affect HF radio propagation conditions, the Harbin Engineering University, the People's Republic of China (PRC), has developed the multi-frequency multipath system based on the software-defined radio technology and designed for obliquely sounding the ionosphere [1 – 7]. The Doppler spectra and amplitudes of the signals reflected from the ionosphere along 14 radio paths have been analyzed (Table 1).

3 Observations

Examples of temporal variations in the Doppler spectra and amplitudes of radio waves reflected in the course of the 25 – 26 August 2018 ionospheric storm (Hwaseong to Harbin and Yamata to Harbin propagation paths), the 5 September 2018 Japan earthquake of Richter magnitude 6.6 (Hwaseong to Harbin and Goyang to Harbin propagation paths), and the 11 August 2018 solar eclipse over the PRC (Hailar to Harbin, Beijing to Harbin, Hohhot to Harbin, and Chiba to Harbin propagation paths) are presented in Figures 1, 2, and 3, respectively. It can be seen that the ionospheric perturbations appreciably affect the HF radio wave characteristics.

Table 1. Basic parameters of the 14 radio paths used for probing the ionosphere at oblique incidence. Retrieved from <https://fmscan.org/index.php>

Frequency [kHz]	Transmitter		Propagation path midpoint	
	North latitude	Location (country)	Distance to Harbin [km]	North latitude
	East longitude [deg]			East longitude [deg]
5,000	34.95 109.56	Lintong/ Pucheng (China)	938	40.37 118.12
6,015	37.21 126.78	Hwaseong (ROK)	475	41.50 126.73
6,055	35.47 140.21	Chiba/ Nagara (Japan)	805	40.63 133.45
6,080	49.18 119.72	Hailar/ Nanmen (China)	323	47.48 123.20
6,175	39.75 116.81	Beijing (China)	525	42.77 121.75
6,600	37.60 126.85	Goyang (ROK)	455	41.69 126.77
7,260	47.80 107.17	Ulaanbaatar / Khonkhor (Mongolia)	748	46.79 116.93
7,295	62.24 129.81	Yakutsk (Russia)	923	54.01 128.25
7,345	62.24 129.81	Yakutsk (Russia)	923	54.01 128.25
9,500	38.47 114.13	Shijia- zhuang (China)	655	42.13 120.41
9,520	40.72 111.55	Hohhot (China)	670	43.25 119.12
9,675	39.75 116.81	Beijing (China)	525	42.77 121.75
9,750	36.17 139.82	Yamata (Japan)	785	40.98 133.25
9,830	39.75 116.81	Beijing (China)	525	42.77 121.75

4 Conclusions

The multi-frequency coherent multipath system for obliquely sounding the ionosphere was utilized for observing disturbances of various origins in the ionosphere over the China area.

1. The $K_{pmax} = 7$ magnetic storm is determined to be accompanied by a strong positive ionospheric storm that persisted for no less than 16 h, from 22:00 UT on 25 August 2018 to 14:00 UT on 26 August 2018. In the course of the storm, an increase in the level of reflection by ~50 – 100 km, as well as oscillations in the reflection

height with amplitude of ~30–40 km, were repeatedly observed along all propagation paths. The uplifting of the levels of reflection was followed by their displacements downward by tens of kilometers. The uplifting and lowering of the levels of reflection were caused by a factor of 1.5–2 decrease and by a factor of a few times increase in the electron density, N , respectively. An increase in N attained a maximum value of 1.5 times in the ionospheric E region and a factor of 3 in the F region. The relative amplitude of the oscillations in N reached many tens of per cent. On the reference days, amplitude of the oscillations in the Doppler shift of frequency was by a factor of a few times less. The oscillations observed in the Doppler shift of frequency were apparently caused by the generation of atmospheric gravity waves in the vicinity of the polar cusp and their subsequent propagation to midlatitudes where the observational instrumentation is located. The wave perturbations had a speed of 275–480 m/s and a period of ~60 min.

2. The character of variations in the Doppler spectrum, the main mode Doppler shift of frequency, and in the signal amplitude observed on the day of a moderate ($M \approx 6.6$) earthquake and on the reference days is detected to be noticeably different. Two characteristic apparent speeds of 3.3 km/s and approximately 500 m/s have been revealed. The former is close to the speed of seismic waves, while the latter is close to the speed of acoustic and atmospheric gravity waves at ionospheric heights. The estimates have shown that perturbations in N caused by infrasonic and atmospheric gravity waves on the day of the earthquake attained ~0.15–0.31% and 7–8%, respectively.

3. The ionospheric response to the partial solar eclipse has been detected and investigated. The eclipse is associated with an increase in the number of rays, the generation of oscillation processes in the atmospheric gravity wave range of periods, with a negative Doppler shift of frequency at first and with a positive shift of smaller magnitude subsequently. The greatest reduction, 26%, in the electron density is determined to occur in the ionospheric E region along the Hailar to Harbin propagation path where the eclipse magnitude of 0.516 and the eclipse obscuration of 0.415 occurred. The magnitude of this decrease determined from the observations virtually does not differ from the theoretical estimates, 24%. The relative amplitude of quasi-periodic oscillations in the electron density during the solar eclipse lies in the range of ~1–10%.

5 Acknowledgements

Work by Qiang Guo and Yu Zheng was supported by National key R & D plan strategic international science and technology cooperation and innovation (2018YFE0206500). Work by L. F. Chernogor and Y. Luo was supported by the National Research Foundation of Ukraine for financial support (project

2020.02/0015, "Theoretical and experimental studies of global disturbances from natural and technogenic sources in the Earth–atmosphere–ionosphere system"). Work by L. F. Chernogor and by V. T. Rozumenko was supported by Ukraine state research project #0119U002538. Work by K. P. Garmash was supported by Ukraine state research project #0118U002039.

6 References

1. Q. Guo, L. F. Chernogor, K. P. Garmash, V. T. Rozumenko, Y. Zheng, "Dynamical processes in the ionosphere following the moderate earthquake in Japan on 7 July 2018," *Journal of Atmospheric and Solar-Terrestrial Physics*, **186**, May 2019, pp. 88–103, <https://doi.org/10.1016/j.jastp.2019.02.003>
2. Q. Guo, Y. Zheng, L. F. Chernogor, K. P. Garmash, V. T. Rozumenko, "Passive HF Doppler Radar for Oblique-Incidence Ionospheric Sounding," *2019 IEEE 2nd Ukraine Conference on Electrical and Computer Engineering*. Lviv, Ukraine, July 2–6, 2019, pp. 88–93, <https://doi.org/10.1109/UKRCON.2019.8879807>
3. L. F. Chernogor, K. P. Garmash, Q. Guo, Y. Zheng, "Effects of the Strong Ionospheric Storm of August 26, 2018: Results of Multipath Radiophysical Monitoring," *Geomagnetism and Aeronomy*, **61**, 1, January 2021, pp. 73–91.
4. L. F. Chernogor, K. P. Garmash, Q. Guo, V. T. Rozumenko, Y. Zheng, "Physical Processes Operating in the Ionosphere after the Earthquake of Richter Magnitude 5.9 in Japan on July 7, 2018," *Astronomy and Space Physics in the Kyiv University. Book of Abstracts. International Conference*. May 28–May 31, 2019, pp. 87–88.
5. L. F. Chernogor, K. P. Garmash, Q. Guo, V. T. Rozumenko, Y. Zheng, "Effects of the Severe Ionospheric Storm of 26 August 2018," *Astronomy and Space Physics in the Kyiv University. Book of Abstracts. International Conference*. May 28–May 31, 2019, pp. 88–90.
6. Q. Guo, Y. Zheng, L. F. Chernogor, K. P. Garmash, V. T. Rozumenko "Ionospheric processes observed with the passive oblique-incidence HF Doppler radar," *Bulletin of Karazin Kharkov National University, "Radiophysics and Electronics" series*, **30**, December 2019, pp. 3–15.
7. Q. Guo, L. F. Chernogor, K. P. Garmash, V. T. Rozumenko, Y. Zheng, "Radio Monitoring of Dynamic Processes in the Ionosphere over China during the Partial Solar Eclipse of 11 August 2018," *Radio Science*, **55**, 2, February 2020, no. e2019RS006866 <https://doi.org/10.1029/2019RS006866>

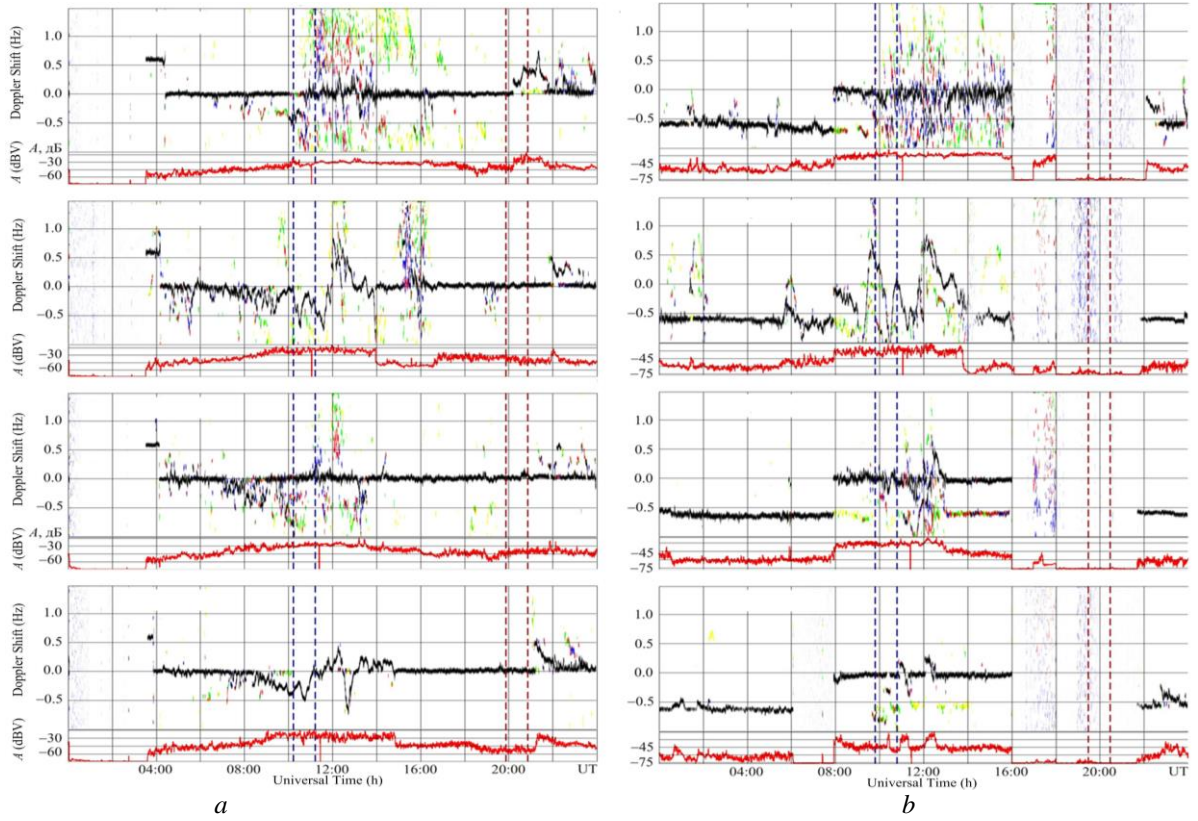


Figure 1. Universal time variations of Doppler spectra and relative signal amplitude, A , for 25, 26, 27 and 28 August 2018 (panels from top to bottom, respectively) along the (a) Hwaseong to Harbin and (b) the Yamata to Harbin propagation paths. Hereinafter, vertical dashed lines show sunrise and sunset times at 0- and 100-km altitude. The signal amplitude, A , at the receiver output in decibels, dBV, relative to 1 V is shown below the Doppler spectrum in every panel

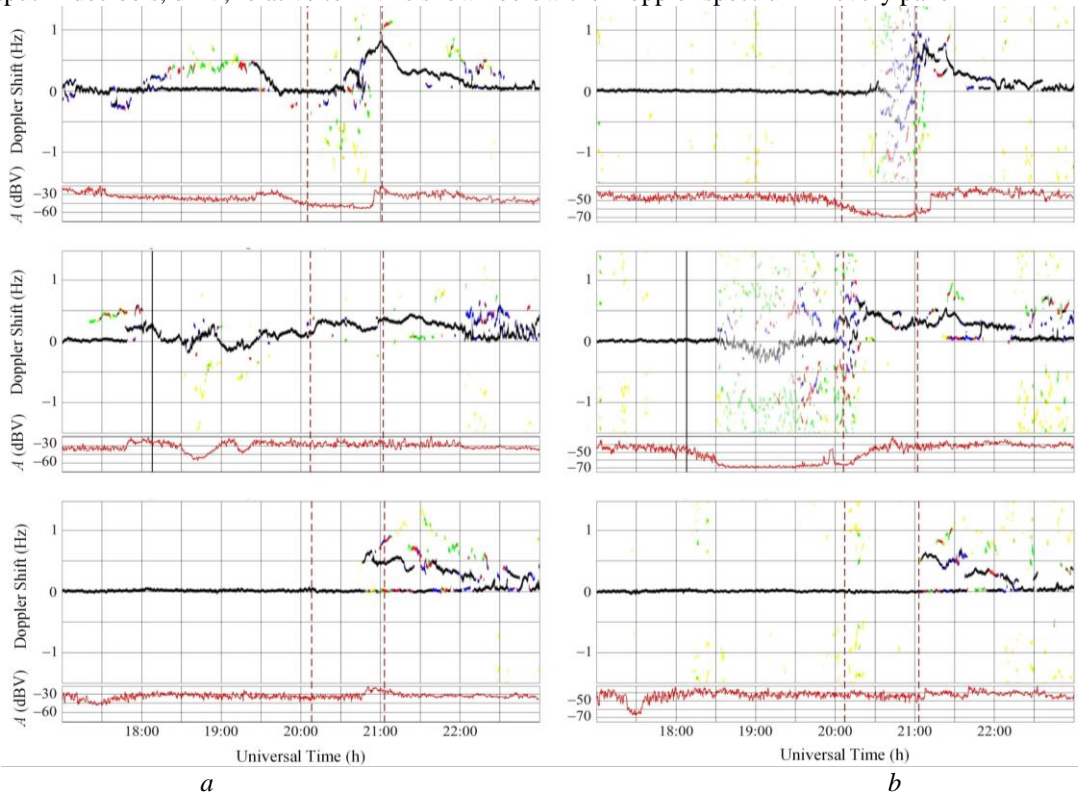


Figure 2. Same as Figure 1, but for 4, 5 and 6 September 2018 for the (a) Hwaseong to Harbin and (b) Goyang to Harbin radiowave propagation paths. The moment when the earthquake occurred is indicated by solid line

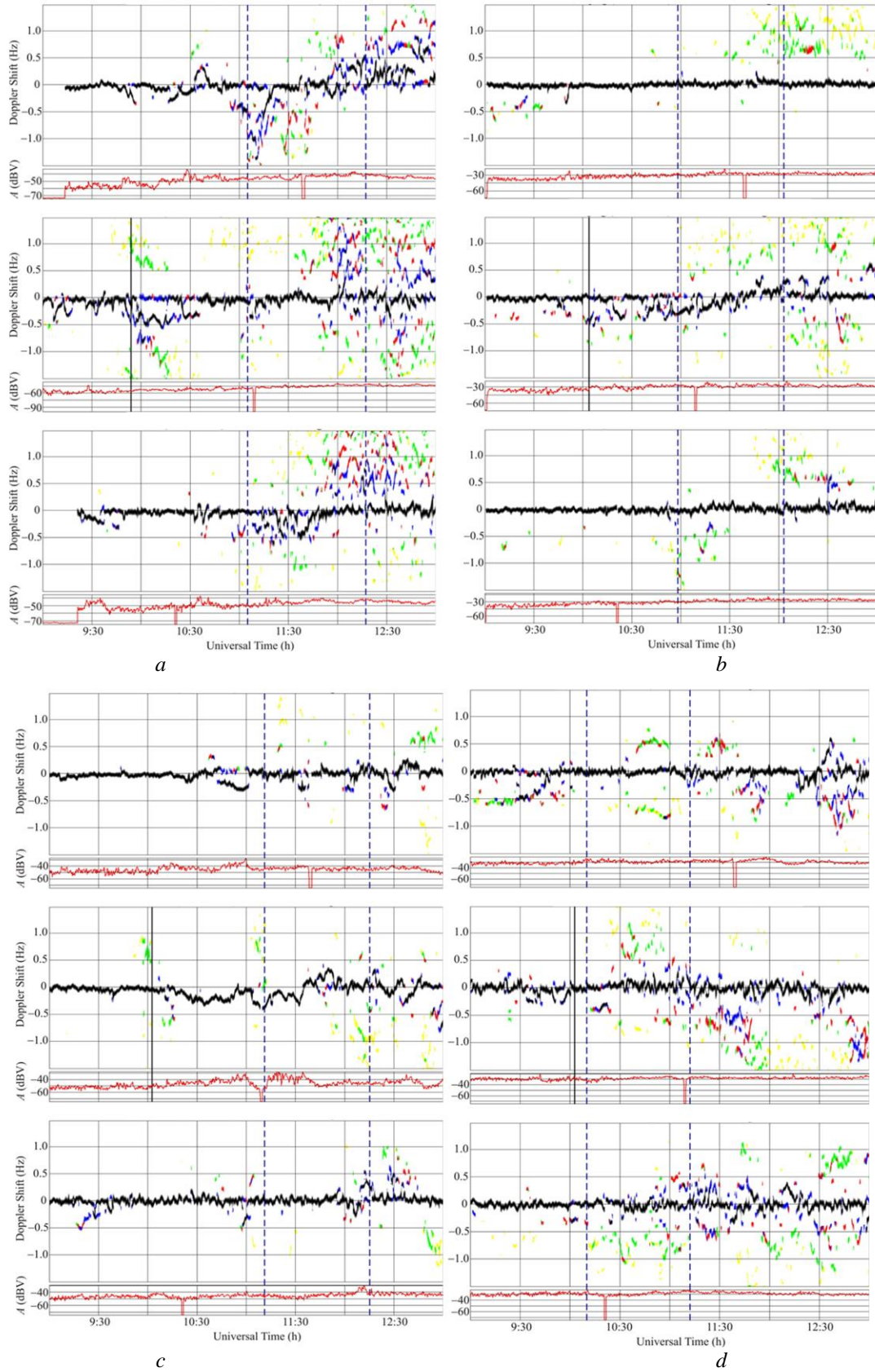


Figure 3. Same as Figure 1, but for 10, 11 and 12 August 2018 (plots from top to bottom, respectively) for the (a) Hailar to Harbin, (b) Beijing to Harbin, (c) Hohhot to Harbin, and (d) Chiba to Harbin radiowave propagation paths. The moment when the solar eclipse occurred at 100-km altitude is indicated by solid line